Annu. Rev. Astron. Astrophys. 1991. 29: 409–45

THE MASS OF THE GALAXY

Michel Fich

Guelph-Waterloo Program for Graduate Work in Physics,
University of Waterloo, Waterloo, Ontario N2L 3G1, Canada

Scott Tremaine

Canadian Institute for Theoretical Astrophysics, University of Toronto,
Toronto, Ontario M5S 1A1, Canada

KEY WORDS: galactic structure, galactic dynamics, dark matter, galactic kinematics, galactic halo, Local Group

1. INTRODUCTION

What is the mass of the Galaxy? The most important recent progress in addressing this question has been the recognition that it is not well-posed. Several related arguments indicate that there is probably no precise and natural definition of the mass of a giant galaxy like our own:

1. Mergers of galaxies are common, so that galaxies grow more massive at an irregular rate. For example, it is likely that both the Magellanic Clouds and the nearby giant galaxy M31 will merge with the Milky Way within 10^{10} yr (see Wielen 1990 for discussions of galaxy mergers).
2. The rotation curves of other galaxies do not exhibit the Keplerian falloff $V(R) \propto R^{-1/2}$ that would be expected in their outer parts if the mass distribution was similar to the distribution of visible stars. Instead, the rotation curves are approximately flat [$V(R)$ = constant], at least out to the radius where the column density of H I becomes too low to detect—which is often more than twice the outer radius of the optically visible galaxy (see Casertano & van Albada 1990 for a review). This result implies that galaxies contain extended halos of dark mass (that is, mass detected only through its gravitational force) outside the distribution of visible stars. The precise extent of these halos is difficult to

0066-4146/91/0915-0409$02.00

measure, as is their shape: They are usually assumed to be spherical for simplicity but in fact are likely to be triaxial and may even be disklike.

3. Inflation and other cosmological arguments suggest that the density of the Universe is near the critical value $\rho_c = 3H^2/(8\pi G)$ at which the kinetic energy associated with the Hubble expansion $v = Hr$ is equal and opposite to the gravitational potential energy $-\frac{4}{3}\pi G\rho r^2$ (see Peebles 1986 for a review). In a universe with near-critical density, extended galactic halos arise naturally from infall of distant material bound to the original protogalaxy (Gunn 1977). For an isolated protogalaxy in a zero-pressure critical universe, the mass bound to the protogalaxy is infinite. In the more realistic case, that of an irregular density field containing many density peaks (potential protogalaxies), halos form first around the highest-density peaks, which then merge with each other and with lower-density structures formed at later times. In such an instance, defining the outer boundary or total mass of a given galaxy is no easier than defining the boundary of a single wave on a stormy sea.

In this review, we discuss the observational constraints on the mass distribution in the outer Galaxy and compare these constraints to simple theoretical models. Because of space constraints, a number of related issues are not discussed. We shall not attempt to evaluate the total mass of the Galaxy. Also, we do not describe detailed models for the distribution of mass within the various visible components (disk, spheroid, etc) of the Galaxy (but see Section 2.5 for references on this subject). Our constraints are not used to set limits on the mass-to-light ratio of the Galaxy for two reasons: (*a*) Little evidence exists that the total mass and total luminosity of galaxies are correlated; (*b*) the total luminosity of the Galaxy is uncertain by about a factor of two [van den Bergh 1988 summarizes recent estimates and arrives at a value $L_B = (2.3 \pm 0.6) \times 10^{10}\ L_\odot$]. Finally, we assume throughout that conventional Newtonian dynamics and gravity are valid; for a review of alternative theories of gravity in the context of galaxy dynamics, see Sanders (1990).

Gilmore et al (1990) provide a good general introduction to Galactic structure.

1.1 *History*

The first systematic efforts to measure the spatial distribution of the stars in the Galaxy were made by William Herschel in the eighteenth century (for historical reviews see Plaskett & Pearce 1936, Berendzen et al 1984, and Paul 1986). By the early twentieth century, Kapteyn (1922) could combine star counts, radial velocities, and proper motions in selected areas

to derive a detailed model of the size and shape of the Galaxy. The so-called Kapteyn Universe was oblate, with an axis ratio of about 5:1, and a semimajor axis of about 8 kpc. Kapteyn also estimated the mass of the Galaxy by using the total number, N, of visible stars as determined from counts, as well as the mean mass per star, $\bar{m}$, as determined by requiring hydrostatic equilibrium normal to the Galactic plane. Kapteyn's results, $N = 4.74 \times 10^{10}$ and $\bar{m} = 1.4$ to $2.2\ M_\odot$, led to a mass $M_G = N\bar{m} = (0.6\text{–}1.0) \times 10^{11}\ M_\odot$, the first plausible estimate of the total mass of the Galaxy. Kapteyn also pointed out that the rough agreement between $\bar{m}$ and the stellar masses derived from binary orbits implied that the dark mass in the Galactic disk could not be much larger than the mass in stars, a conclusion that remains valid today. Unfortunately, Kapteyn neglected interstellar absorption and hence the size and shape of Kapteyn's Universe, as well as the position of the Sun near its center, reflects the effects of absorption more than the actual geometry of the Galaxy.

The modern view of our Galaxy originates with Harlow Shapley's discovery that the Sun is not at its center. Shapley (1918) found that the globular cluster system of our Galaxy is centered on a point 13 kpc away from the Sun and inferred that this was the center of the Galaxy. This was the first estimate of the Sun's Galactocentric distance, R_o, one of the fundamental parameters describing the scale of the Galaxy. Later, after interstellar absorption was discovered from observations of open clusters (Trumpler 1930), the distances to the globular clusters were reevaluated; Stebbins & Whitford (1936) arrived at values of R_o in the range 7.6 to 8.4 kpc, close to current estimates (see below).

A second fundamental parameter is the rotation rate of the Local Standard of Rest (LSR) around the center of the Galaxy, denoted Θ_o. Crudely, the LSR is a fictional point at the Sun's present position that travels at the mean velocity of the stars in the solar neighborhood. This definition is crude because stellar populations with larger velocity dispersions generally have smaller mean velocities (the asymmetrical drift); a more accurate definition is that the LSR travels at the mean velocity of a stellar population with negligible dispersion. The velocity of the Sun relative to the LSR (the solar motion) is computed in practice by plotting the velocity of the Sun relative to stellar populations with various dispersions and extrapolating to zero dispersion (see Mihalas & Binney 1981, Section 6.4).[1]

Lindblad (1926) first attempted to model the rotation of the Galaxy.

[1] The definition of Θ_o assumes that the LSR travels in a circular orbit around the Galactic center; in fact, this is only an approximation because the Galaxy is not exactly axisymmetric because of spiral structure and possible large-scale distortions. The LSR may have a radial velocity of up to 5% or more of the circular speed (see Section 2.4).

He argued that the Galaxy was composed of several subsystems rotating about an axis normal to the plane of the Milky Way, with a common center defined by the globular cluster system. The subsystems differed in their rotational speed and degree of flattening, ranging from the globular clusters, which were spherically distributed with a small rotation speed, to the system containing the Sun and the Cepheids, which was highly flattened and rapidly rotating. To explain Kapteyn's star counts, Lindblad argued that the Kapteyn Universe was only a small star cloud, orbiting inside a larger disk with dimensions similar to those of the globular cluster system. With this model Lindblad successfully explained the asymmetric distribution of the mean velocities of stars and clusters; he also derived a mass for the Galaxy of $1.8 \times 10^{11}\ M_\odot$ by balancing the gravitational attraction of the Galaxy against the centrifugal force on the Sun.

The modern treatment of the effect of the Galaxy's rotation on nearby stars began with Oort (1927). Oort assumed that the mean velocity of the stars in a given volume element at distance R from the Galactic center corresponds to rotation with velocity $\Theta(R)$, that the stars we observe are all relatively close to the Sun ($|R-R_o| \ll R_o$), and that the equations describing the relative motions due to differential rotation can be replaced by first-order approximations in $|R-R_o|/R_o$. The mean radial velocity v_r and proper motion μ of a group of stars at Galactic longitude ℓ and distance d from the sun is then

$$v_r = Ad \sin 2\ell, \quad \mu = A \cos 2\ell + B, \tag{1.}$$

where the Oort constants A and B are given by

$$A = \frac{1}{2}\left(\frac{\Theta}{R} - \frac{d\Theta}{dR}\right)_{R_o}, \quad B \equiv -\frac{1}{2}\left(\frac{\Theta}{R} + \frac{d\Theta}{dR}\right)_{R_o}. \tag{2.}$$

The values of the A and B constants, which measure the local shear and vorticity respectively, can be derived from local measurements of radial velocity and proper motion, and constrain the values of Θ_o, R_o, and $(d\Theta/dR)_{R_o}$. Using $R_o = 6$ kpc and a circular speed $\Theta_o = 272\ \mathrm{km\ s^{-1}}$ derived from the difference between the mean velocities of the globular clusters and local disk stars [from data of Strömberg (1918, 1925)], Oort (1927) estimated the mass of the Galaxy to be at least $8 \times 10^{10}\ M_\odot$.

Bucerius (1934) was the first to model the distribution of mass throughout the Galaxy and fit this density distribution to the local rotation parameters. His model used a disk density distribution with $R_o = 10$ kpc and $\Theta_o = 278\ \mathrm{km\ s^{-1}}$ to derive a Galactic mass of $2.4 \times 10^{11}\ M_\odot$. Plaskett & Pearce (1936) analyzed the radial velocities and proper motions of O and B stars to measure the local rotation constants. Using $R_o = 10$ kpc and

$\Theta_o = 275$ km s^{-1}, they estimated the mass of the Galaxy to be 1.65×10^{11} $M_\odot$.

The mass distribution of the Galaxy can be determined more accurately by sampling objects throughout the Galaxy rather than just near the Sun. Camm (1938) showed that in a differentially rotating disk the radial velocity of an object relative to the LSR is given by

$$v_r = \left[\frac{\Theta(R)}{R} - \frac{\Theta_o}{R_o}\right] R_o \sin \ell, \qquad 3.$$

where $\Theta(R)$ is the circular velocity at the Galactocentric distance R of the object and ℓ is its Galactic longitude. Camm analyzed a sample of planetary nebulae, which are visible at great distances because of their strong emission lines. Using both proper motions and radial velocities, he found $R_o = 9.83 \pm 0.11$ kpc, $\Theta_o = 195 \pm 43$ km s^{-1}, and estimated the mass to be 1.77×10^{11} $M_\odot$. Since Camm's work, the planetary nebulae have not received much attention as tracers of Galactic structure because of concern about uncertainties in their distances and incompleteness due to absorption (but see Schneider & Terzian 1983).

The study of Galactic structure was revolutionized by the discovery of 21-cm line emission from interstellar atomic hydrogen (H I) in the Galactic disk (see Burton 1988 for a review). Because the Galaxy is largely transparent at this wavelength, astronomers for the first time were able to map the global distribution and kinematics of a single component of the disk. Unfortunately, it is usually impossible to determine the distance to a given H I cloud, so Equation 3 cannot be applied. However, for a given longitude $|\ell| < 90°$, provided $\Theta(R)/R$ decreases outwards (as is almost always true), the maximum radial velocity of any material in the disk can be shown from Equation 3 to be

$$v_{max} = \Theta(R_o \sin \ell) - \Theta_o \sin \ell, \qquad 4.$$

By measuring the maximum velocity at which H I emission is detected (the tangent point method), the rotation curve can be determined for $R < R_o$ so long as Θ_o and R_o are known.

Once H I rotation curves became available by this method, numerous astronomers investigated the mass distribution of the Galaxy. In general these were all attempts to find a mass distribution that resulted in reasonable fits to the global H I data and the local data for objects near the Sun. Perek (1962) summarized much of this work. These efforts culminated in the review by Schmidt (1965). Schmidt's estimate of the mass of the Galaxy was 1.8×10^{11} $M_\odot$. His model for the mass distribution and the accompanying estimates for the rotation parameters were widely accepted

for many years, in part because IAU Commission 33 recommended the adoption of Schmidt's values of

$$R_\odot = 10\,\mathrm{kpc}, \quad \Theta_\odot = 250\,\mathrm{km\,s^{-1}}, A = 15\,\mathrm{km\,s^{-1}\,kpc^{-1}},$$
$$\text{and} \quad B = -10\,\mathrm{km\,s^{-1}\,kpc^{-1}} \quad 5.$$

as the "official" standard (Pecker 1964).

Substantial improvements to Schmidt's model only began to appear in the late 1970s; these more recent models of the Galaxy are discussed in Section 2.5.

1.2 *Rotation Parameters*

The four so-called rotation parameters $\Theta_\odot$, $R_\odot$, A, and B play an important role in almost all determinations of the rotation curve and mass distribution in the Galaxy. Only three of the four are independent because $A-B = \Theta_\odot/R_\odot$. Because rotation with uniform angular speed leaves distances invariant, any rotation curve determined from radial velocity data alone is undetermined up to the addition of a component ΩR for arbitrary fixed Ω. Thus, in order to derive a unique rotation curve from radial velocity measurements, additional information is needed—usually in the form of values of one or more of the rotation parameters. Differences between published rotation curves often arise from the choice of these parameters rather than from differences in the data.

Estimates of the rotation parameters have continued to evolve since the IAU's adoption of Schmidt's values in 1964. The most recent major review by Kerr & Lynden-Bell (1986) estimates $R_\odot = 8.5 \pm 1.1$ kpc, $\Theta_\odot = 222 \pm 20$ km s^{-1}, $A = 14.4 \pm 1.2$ km s^{-1} kpc^{-1}, $B = -12.0 \pm 2.8$ km s^{-1} kpc^{-1}, and $A-B = 26.4 \pm 1.9$ km s^{-1} kpc^{-1}. The errors in these estimates are stongly correlated because the observations often constrain combinations of the rotation parameters. For example, the shape of the velocity ellipsoid for old disk stars determines $B/(B-A)$, and the derivative $dv_{\max}/d(\sin \ell)$ at $|\ell| = 90°$ determines $AR_\odot$ (see Equations 2 and 4).

Figure 1 illustrates how four of the quantities determined from local observations constrain the circular speed $\Theta_\odot$ and its gradient $(d\Theta/dR)_{R_\odot}$. Using the means and standard deviations (σ) given by Kerr & Lynden-Bell (1986), we plot constraints from A and B (measured from radial velocities and proper motions of nearby stars respectively), $AR_\odot$ (from $dv_{\max}/d\sin\ell$), and $B/(B-A)$ (from the velocity ellipsoid). Each area element on the plots is shaded with a gray scale ranging from 0 (white) to 8 (darkest); each constraint contributes 1 to the gray scale if the elcmcnt lies outside 1σ and 2 if it lies outside 2σ. We have not included constraints arising from direct measurements of $R_\odot$ or $\Theta_\odot$ because these are not local

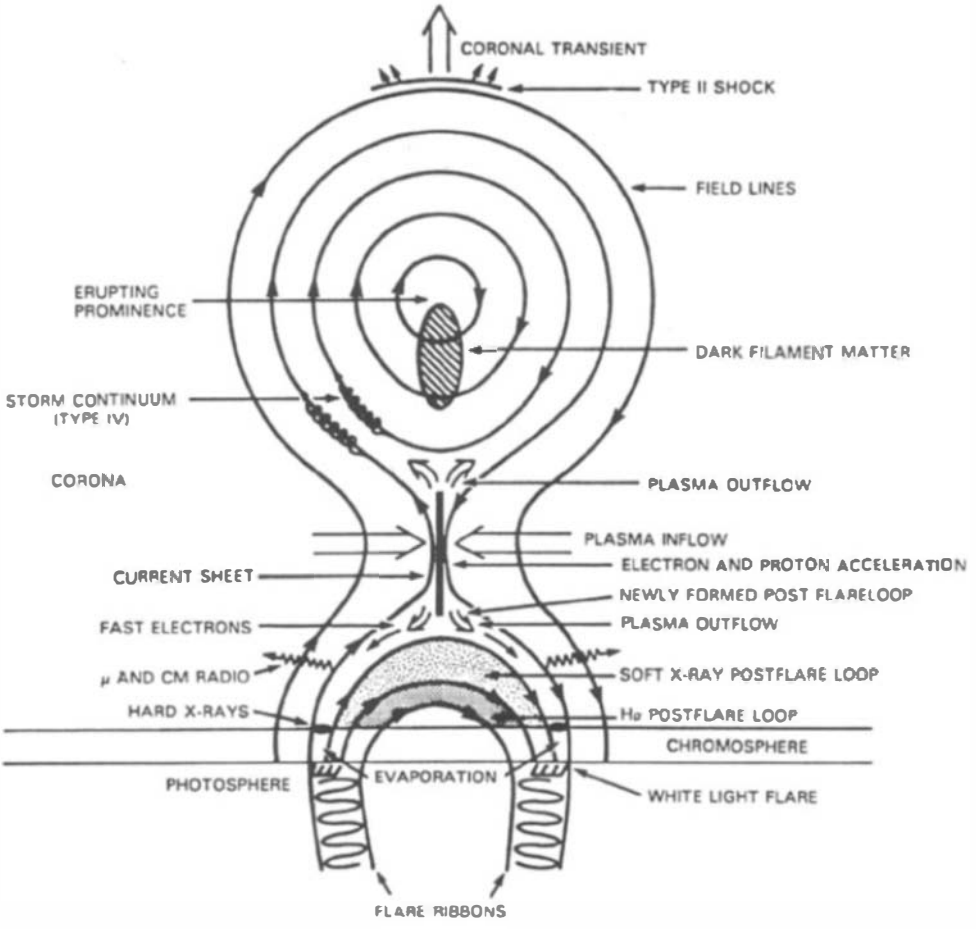

Figure 1 Constraints on the local circular speed Θ_o and its gradient $(d\Theta/dR)_{R_o}$ from measurements of Oort's A constant obtained from radial velocities, $A = 14.5 \pm 1.3$ km s^{-1} kpc^{-1} (*solid lines*), Oort's B constant from proper motions, $B = -12.0 \pm 2.8$ km s^{-1} kpc^{-1} (*short-dashed lines*), $AR_o = 124.5 \pm 17$ km s^{-1} as determined from the slope of the terminal velocity curve as a function of $\sin \ell$ (*long-dashed lines*), and $B/(B-A) = 0.42 \pm 0.06$ as determined from the velocity ellipsoid (*dash-dot lines*). Heavy lines denote 1σ limits and lighter lines denote 2σ limits. Means and standard deviations are taken from Kerr & Lynden-Bell (1986). One unit is contributed to the gray scale for each constraint that is violated at the 1σ level, two units for constraints violated at the 2σ level. Constraints arising from direct determinations of R_o or Θ_o are not shown.

measurements. Several conclusions can be drawn from the Figure. (*a*) A flat or rising rotation curve, $(d\Theta/dR) \geq 0$, is ruled out at the 1.3σ level for all R_0 by measurements of the velocity ellipsoid. We shall argue below that the rotation curve is nearly flat, which suggests that the determination of rotation constants from the velocity ellipsoid is suspect, perhaps because of nonaxisymmetric motions or failure of the epicycle approximation (Binney 1987). (*b*) Small values of R_0 (say, $R_0 = 7$ kpc) are associated with small values of Θ_0 and are difficult to reconcile with a flat rotation curve even if the velocity ellipsoid constraint is ignored. (*c*) The constraints from B are largely irrelevant if the rotation curve is nearly flat. (*d*) Neither R_0 nor Θ_0 is well-constrained by these local measurements; thus the reliability of the rotation parameters, and hence of the rotation curve, requires accurate direct measurements of R_0 and Θ_0.

Following the review of Kerr & Lynden-Bell, IAU Commission 33 recommended use of the values

$$R_0 = 8.5\,\text{kpc} \quad \text{and} \quad \Theta_0 = 220\,\text{km}\,\text{s}^{-1} \qquad 6.$$

to facilitate intercomparison of the work of different authors (Swings 1985). We use these values wherever possible in this review. The IAU Commission made no recommendation concerning A and B.

Some new methods and results have appeared since these recommendations were made. Currently the most promising approach to determining R_0 is through the measurement of proper motions and radial velocities of H_2O maser spots. The spots in a given source appear to be expanding outwards from a common center; if the outflow is assumed to be spherical, the ratio of the rms proper motion to the rms radial velocity yields a measurement of the distance. Reid et al (1988b) analyzed the motions in the source Sgr B2(N), which lies close to the Galactic center, to determine that $R_0 = 7.1 \pm 1.5$ kpc. The source W49(N) yields a similar result, $R_0 = 7.6 \pm 1.6$ kpc (Gwinn et al 1989). The most recent review on R_0 combines determinations by all methods and arrives at a best value of $R_0 = 7.7 \pm 0.7$ kpc (Reid 1989). A reanalysis of the distribution of color excesses and horizontal branch magnitudes in highly reddened globular clusters near the Galactic center (Racine & Harris 1989) yields a similar result, $R_0 = 7.5 \pm 0.9$ kpc. Thus the preferred values of R_0 have steadily declined over the past two or three decades (from the 1964 IAU value of 10 kpc to the 1985 IAU value of 8.5 kpc to the present value of 7–8 kpc).

The H_2O maser method should also lead to a more accurate value of Θ_0 by measuring the proper motion of sources relative to the extragalactic background (Reid et al 1988a); moreover, in the future VLBI arrays should be able to measure the trigonometric parallax of the source Sgr A at the Galactic center to obtain a geometric measurement of R_0.

Another promising project is the Lick Northern Proper Motion Program [see Hanson (1988) for a review]. Hanson (1987) presented first results of this study and found $A = 11.31 \pm 1.06$ km s^{-1} kpc^{-1} and $B = -13.91 \pm 0.92$ km s^{-1} kpc^{-1}—consistent with the current IAU values of R_o and Θ_o (Hanson's result is $\Theta_o/R_o = A - B = 25.22 \pm 1.40$ km s^{-1} kpc^{-1} compared with the IAU value 25.88 km s^{-1} kpc^{-1}). Hanson's result implies that the rotation curve rises locally. On the other hand, a recent study of the kinematics of late-type supergiants gives a much higher value of 16 ± 1.5 km s^{-1} kpc^{-1} for A (Dubath et al 1988). The reasons for the large spread in values of A are unknown but may include systematic distance errors, differences in the sample volume, or poorly understood kinematic differences between the older stellar population used in Hanson's study and the younger population used by Dubath et al (see Lewis 1990).

The *HIPPARCOS* astrometric satellite launched by ESA in August 1989 suffered a serious setback when the apogee boost motor failed, leaving the satellite in a transfer orbit. At present (September 1990) it appears that most of the mission goals can still be achieved, including the measurement of some 10^5 stellar parallaxes at the level of 0.002 arcsec. A successful *HIPPARCOS* mission should greatly enhance our understanding of the kinematics of the stars in the solar neighborhood and thereby will improve both the rotation parameters and our overall understanding of Galactic structure.

2. THE ROTATION CURVE

2.1 *Methods*

To measure the rotation curve of the Galaxy we need radial velocities for a set of disk objects that occupy a large range of Galactocentric distance R. The most accurate velocities are obtained from the bright narrow lines found at millimeter wavelengths.

Candidate objects must be bright enough to be visible at large distances, possess good distance indicators, and have well-determined radial velocities. A variety of objects has been used: carbon stars (Schechter et al 1988), planetary nebulae (Schneider & Terzian 1983), Cepheids (Caldwell & Coulson 1987, Welch 1988), and HII regions (Moffat et al 1979, Blitz 1979).

Some approaches circumvent the need for distances. The most important is the tangent point method (Equation 4), which is the usual approach to measuring the rotation curve for $R < R_o$ from observations of cold gas (HI or CO). However, the tangent point method cannot measure the outer rotation curve ($R > R_o$). Also, by focusing exclusively on the maximum

velocity at a given longitude, this method ignores most of the available information in the radial velocity vs longitude plane.

An alternative approach fits the complete distribution of brightness temperature as a function of longitude and radial velocity (integrated over latitude) to an axisymmetric Galaxy model in which the rotation curve $\Theta(R)$ and H I surface density $\Sigma(R)$ are free functions.[2] This method has not been widely used, in part because it appears to be sensitive to deviations from axisymmetry (Petrovskaya & Teerikorpi 1986).

A third distance-independent approach is to assume that the H I surface density distribution is exponential, $\Sigma(R) = \Sigma_0 \exp(-\lambda R/R_0)$, similar to the distributions seen in other galaxies. The free parameter λ is determined by fitting the distribution in the inner Galaxy ($R < R_0$), using the rotation curve determined by the tangent point method; then the rotation curve for $R > R_0$ can be found by fitting the brightness temperature as a function of radial velocity for longitudes that sample the outer Galaxy (see Knapp 1988 for a review).

2.2 *Inner Galaxy Results*

Although we are mainly interested in the mass distribution in the outer Galaxy ($R > R_0$), we give a brief summary of measurements of the rotation curve of the inner Galaxy. All of the studies described below use the tangent point method.

Kwee et al (1954) carried out an influential early study of the northern ($0° < \ell < 90°$) H I rotation curve. They determined the velocities v_{max} in Equation 4 by fitting the brightness temperature profiles to models with a spatially uniform H I distribution and a Maxwellian distribution of random velocities. Their rotation curve exhibited oscillations with an amplitude of about 10 km s^{-1}; they attributed these oscillations to the absence of H I at the tangent point along some lines of sight, and hence drew their smoothed rotation curve through the maxima of the oscillations. However, the oscillations almost certainly arise from local irregularities in the H I velocity field, possibly resulting from spiral structure, so it is more plausible to draw a smoothed rotation curve through the mean of the oscillations (Shane & Bieger-Smith 1966).

Subsequently, the southern rotation curve ($270° < \ell < 360°$) was measured in Australia (Kerr 1962, 1964). The northern and southern curves

[2] To see how this is done, note that Equation 3 shows that all points with the same value of $v_r/\sin\ell \equiv \omega$ correspond to the same Galactocentric distance $R(\omega)$, where $R(\omega)$ is the solution of the equation $\omega = R_0\Theta(R)/R - \Theta_0$. By fitting the variation in brightness temperature with longitude along a line $\omega = \text{const}$, one can determine $R(\omega)$ and thereby $\Theta(R)$, so long as Θ_0 and R_0 are known.

were similar in gross appearance, but over much of their range (in R), the northern curve appeared to be higher than the southern by approximately 10 km s^{-1} (see Section 2.4).

Recent analyses of the inner Galaxy rotation curve can be found in Burton & Gordon (1978), Sinha (1978), Clemens (1985), and Rohlfs et al (1986). The inner rotation curve is shown in Figure 2 for the 1985 IAU values of R_o and Θ_o.

2.3 *Outer Galaxy Results*

The failure of the tangent point method for $R > R_o$ greatly complicates the determination of the rotation curve of the outer Galaxy. Early measurements of the outer rotation curve using H II regions, Cepheids, and OB stars (see Georgelin & Georgelin 1970 and references therein) extended only to about $1.3R_o$, which is not far enough to rule out the Schmidt (1965) rotation curve.

A major step forward was the determination of distances to many H II regions using main-sequence fitting in the accompanying stellar associations (Moffat et al 1979). These results permitted Jackson et al (1979) to measure the rotation curve out to about $1.6R_o$. They pointed out that the rotation was quite inconsistent with Schmidt's prediction and that in fact the rotation speed appeared to rise outside R_o rather than exhibiting the Keplerian falloff $\Theta(R) \propto R^{-1/2}$ predicted by the Schmidt model.

Using more accurate radial velocities from CO in molecular clouds associated with the H II regions, Blitz (1979) also found that the rotation curve rose, by about 10% between R_o and $1.6R_o$ (assuming the 1964 IAU values $R_o = 10$ kpc and $\Theta_o = 250$ km s^{-1}). This work was extended to more H II regions and larger distances by Blitz et al (1980, 1982) with similar results. Schneider & Terzian (1983) used planetary nebulae to derive the rotation curve in the outer Galaxy and confirmed the rise. Chini & Wink (1984) measured distances and velocities for a sample of distant H II regions and found an even steeper rise than in the earlier work. However, their distances appear to be systematically larger than those determined by other authors (Fich et al 1989). Initial results using carbon stars (Schechter et al 1988; see also Aaronson et al 1989, 1990) have indicated a flat rotation curve in the outer Galaxy (if $\Theta_o = 250$ km s^{-1}), but within the uncertainties, the results are consistent with the rising rotation curves observed by other authors. Preliminary results from Cepheids appear to yield a similar rotation curve as well (Welch 1988).

The shape of the rotation curve depends on the assumed rotation parameters R_o and Θ_o. If, for example, the value of Θ_o is increased by $\Delta\Theta_o$, the circular speed will change by $\Delta\Theta(R) = \Delta\Theta_o(R/R_o)$. Thus a decrease in Θ_o tends to convert a rising rotation curve into a flat or falling one; an

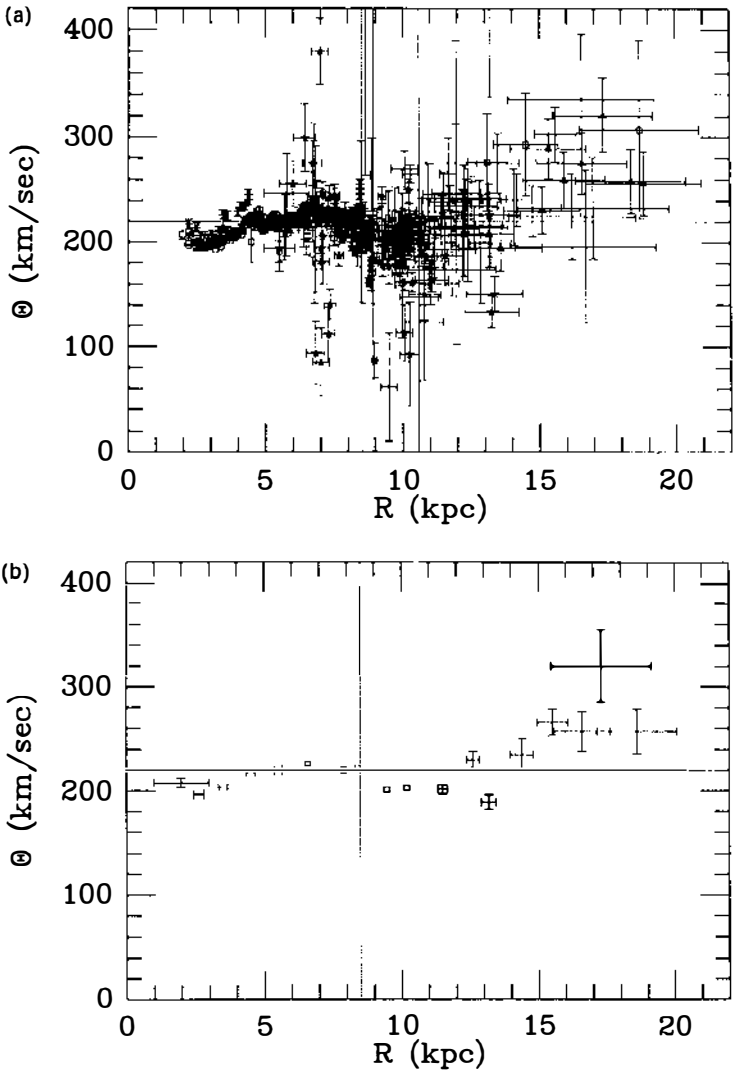

Figure 2 The rotation curve of the Galaxy for the 1985 IAU values $R_o = 8.5$ kpc, $\Theta_o = 220$ km s^{-1} (*dotted lines*). (*a*) Individual data points and associated error bars. Open squares: planetary nebulae from Schneider & Terzian (1983); open circles: CO tangent points from Clemens (1985); open triangles: H II regions from Chini & Wink (1985); stars: open clusters from Hron (1987); asterisks: H I tangent points from Burton & Gordon (1978); naked error bars: H II regions from Fich et al (1989). (*b*) Averaged rotation curve using data in (*a*). The error bars are plotted using the overly optimistic assumption that errors in R and Θ, as well as errors in different data points, are all Gaussian and uncorrelated. Open squares denote cases in which the error bar is smaller than the size of the symbol. Errors in distances determined by the tangent point method are taken to be 1 kpc.

increase in R_o has a similar but weaker effect (e.g. Fich et al 1989). With the change from the 1964 IAU values ($R_o = 10$ kpc, $\Theta_o = 250$ km s^{-1}) to the 1985 values ($R_o = 8.5$ kpc, $\Theta_o = 220$ km s^{-1}), the rising rotation curves claimed for the outer Galaxy in the period 1979–1984 become nearly flat.

In a recent reanalysis of the data from H II regions, using the 1985 IAU rotation parameters, Fich et al (1989) estimated that the rotation curve is flat to within 2% between R_o and $2R_o$, although the uncertainty in the circular speed at $2R_o$ is about 20%. Some evidence suggests a rise in circular speed of 10–20% outside $1.5R_o$. Hron (1989) has argued that OB star distances in the outer Galaxy may be overestimated because of the Galactic metallicity gradient; correcting for this effect could eliminate this apparent rise in circular speed. However, recent work by Fich & Silkey (1991) indicates that the metallicity gradient in the outer Galaxy may be significantly smaller than that used by Hron.

Figure 2 summarizes rotation curve data taken from the literature just discussed. The Figure shows that the rotation curve does not decline for $R > R_o$, implying the presence of significant amounts of mass in the outer Galaxy. Much of the data indicates that the rotation curve continues to rise beyond R_o. Decreasing R_o increases the rise in Θ versus R while decreasing Θ_o has the opposite effect.

2.4 *Noncircular Motions*

The asymmetry between the northern and southern rotation curves was first discussed by Kerr (1962, 1964) who ascribed this observation to an outward motion of the LSR relative to the Galactic center of 7 km s^{-1}. If correct, Kerr's result implies either that (*a*) the usual determinations of the solar motion relative to the LSR are flawed, or that (*b*) the Galaxy as a whole is expanding on a timescale of $R_o/7$ km s$^{-1} = 1 \times 10^9$ yr, which seems unlikely, or that (*c*) the mass distribution and mean velocity field of the Galaxy are nonaxisymmetric. It remains unclear whether the asymmetry results from small-scale perturbations, perhaps from spiral structure, or a large-scale distortion, perhaps due to a triaxial bulge or halo.

As a conceptual aid, we may define the Rotational Standard of Rest (RSR; Shuter 1982), which is a fictional point at the Sun's position that travels in a circular orbit around the Galactic center.[3] Demanding that the spatial and kinematic H I distribution be consistent with axisymmetry fixes

[3] The notations in the literature are not consistent. What we have called the Local Standard of Rest or LSR (the frame moving with the mean velocity of the nearby stars) is sometimes called the "kinematical" LSR, while what we have called the RSR is called the "dynamical" LSR; also, some authors use the term Local Standard of Rest to denote what we call the RSR.

the solar motion with respect to the RSR, while observations of local stellar kinematics fix the solar motion with respect to the LSR. Kerr's result then implies that the LSR and RSR do not coincide.

However, this approach is not really self-consistent: Since the existence of a difference between the LSR and RSR suggests that the Galaxy is nonaxisymmetric, it is inappropriate to demand that the H I distribution be consistent with axisymmetry. A better approach is to fit the observations to dynamically consistent nonaxisymmetric models of the Galaxy that predict both the motion of the LSR and the spatial and kinematic H I distribution (e.g. Blitz & Spergel 1991).

At present, the situation is confused: Strong evidence remains that a stationary, axisymmetric Galaxy with the conventional LSR is inconsistent with the data, but there is little agreement on an improved model. For example, some recent studies (Sinha 1978, Rohlfs et al 1986) of the inner Galaxy rotation curve have questioned Kerr's north-south asymmetry, while other studies have found asymmetries that indicate differences of up to 11 km s^{-1} between the RSR and the LSR (Shuter 1982 using H I; Clemens 1985 using CO; Fich et al 1989 using H II regions).

A recent review and analysis of much of the data can be found in Blitz & Spergel (1991), who argue that the deviations from axisymmetry result from a triaxial spheroid inside the solar circle. In their model, the LSR is receding from the Galactic center at 14 km s^{-1}, while the outermost gas in on nearly circular orbits. Most current theories of galaxy formation imply that galactic halos are generally triaxial (Lin et al 1965, Bardeen et al 1986, Aguilar & Merritt 1990), so it is surprising that the inner Galaxy is nonaxisymmetric while the outer Galaxy is axisymmetric. An alternative interpretation is that the dominant asymmetry is a lopsided distortion ($m = 1$) in the outer Galaxy (Kuijken 1991).

2.5 *The Mass Distribution from the Rotation Curve*

Modern models of the mass distribution in the Galaxy differ from those of Schmidt (1965) and his predecessors in at least two important ways:

1. An important constraint is that the photometric and kinematic properties of the Galaxy should resemble those of other galaxies. Thus the mass distribution in the inner Galaxy arises largely from disk and spheroidal components with photometric properties and mass-to-light ratios similar to those seen in other galaxies.
2. As we have seen, the rotation curve of the Galaxy is flat or rising out to $\gtrsim 2R_o$, and similar behavior is seen in the rotation curves of other spiral galaxies (Casertano & van Albada 1990). The gravitational force from the visible disk and spheroidal components cannot produce a

rotation curve with this shape. Thus most models of the Galaxy contain an invisible mass component extending to large distances (the dark halo) to ensure that the rotation curve remains flat.

The models of Rohlfs & Kreitschmann (1988) are typical of those presented recently. Their models contain three to five components: a disk and spheroid whose parameters are chosen to match photometry of other spiral galaxies, a central component that reproduces infrared photometry of the Galactic center region, and components such as a dark halo that are needed to reproduce features of the rotation curve. They fit their models to the rotation curve using their own estimates of the rotation constants ($R_\odot = 7.9$ kpc, $\Theta_\odot = 185$ km s^{-1}) rather than the IAU values. The total mass of the Galaxy diverges because the extent of the dark halo is not constrained by the rotation curve; within a sphere of radius 50 kpc, the contained mass is in the range (4–14) $\times 10^{11}\ M_\odot$, almost all of which is in the dark halo.

Other influential mass models have been constructed by Innanen (1973), Bahcall & Soneira (1980), Caldwell & Ostriker (1981), and Bahcall et al (1983). Schmidt (1985) gives a brief review, and Rohlfs & Kreitschmann (1988) also list a number of papers on this subject.

3. THEORETICAL MASS MODELS

The models of the mass distribution described in Section 2.5 concentrate on accurate fits to all of the available observations—which mostly constrain the properties of the inner Galaxy ($R < R_\odot$). This review, however, focuses on the mass distribution in the outer Galaxy, where the relevant observations are fragmentary and often difficult to interpret. Thus, instead of making detailed fits or searching for a single best model, we shall compare the observations to three simple representative models of the distribution of mass in the outer Galaxy.

3.1 *The WYSIWYG ("what you see is what you get") Model*

As the acronym implies, the mass distribution is derived from the assumption that the mass density ρ is everywhere proportional to the optical luminosity density j, which almost entirely results from stars. The constant of proportionality is the mass-to-light ratio ρ/j. The luminosity density can be derived using fitting formulae that work well for other galaxies (usually de Vaucouleurs' $R^{1/4}$ law for the spheroid and Freeman's exponential law for the disk) and by fitting the free parameters of the formulae to star count and other data (see de Vaucouleurs & Pence 1978, Bahcall

& Soneira 1980, and Bahcall 1986). Most of the luminosity is interior to the solar radius (about 70% according to Bahcall & Soneira 1980), so the rotation curve is approximately Keplerian at distances well beyond the solar radius (say, $\gtrsim 1.7R_\odot$); thus we may write the mass of the Galaxy as

$$M_G = f\frac{\Theta_\odot^2 R_\odot}{G}, \qquad 7.$$

where the dimensionless factor f is close to unity. For the Bahcall & Soneira (1980) model $f = 1.1$; f depends mainly on the ratio $R_\odot/R_d$, where R_d is the e-folding length of the exponential disk (see Figure 2–17 of Binney & Tremaine 1987). Using the IAU 1985 standard values for $R_\odot$ and $\Theta_\odot$, the WYSIWYG model predicts

$$M_G = 9.5 \times 10^{10} f \left(\frac{\Theta_\odot}{220\ \mathrm{km\ s^{-1}}}\right)^2 \left(\frac{R_\odot}{8.5\ \mathrm{kpc}}\right) M_\odot. \qquad 8.$$

This model is presented as a contrast to more realistic models rather than as a serious attempt to fit the data. It is inconsistent with the rotation curve data because it predicts that well outside the solar radius the rotation speed should be

$$\Theta(R) = \Theta_\odot f^{1/2} (R_\odot/R)^{1/2}. \qquad 9.$$

With $f = 1.1$ and the IAU rotation parameters, the WYSIWYG model predicts $\Theta(2R_\odot = 17\ \mathrm{kpc}) = 163\ \mathrm{km\ s^{-1}}$, far below the data shown in Figure 2.

3.2 *The Minimal Halo Model*

A simple model that produces a flat rotation curve is one in which the mass is spherically distributed, with the mass inside radius r given by[4]

$$M(r) = \begin{cases} \Theta_c^2 r/G, & \text{for } r < r_{\max}, \\ \Theta_c^2 r_{\max}/G \equiv M_G & \text{for } r > r_{\max}. \end{cases} \qquad 10.$$

The sharp cutoff at $r_{\max}$ is unrealistic, but to distinguish between a sharp cutoff and a more realistic gradual one is difficult given the data available.

The rotation curves of other galaxies are generally flat out to the largest radius where H I is detectable, which is two or more times the radius of the outer edge of the optically visible galaxy (e.g. Casertano & van Albada 1990). Thus the smallest plausible halo would have $r_{\max}$ equal to around $3R_{25}$, where R_{25} is the usual measure of the optical edge of the galaxy (blue

[4]We use r to denote radius in spherical coordinates (r, θ, ϕ), in contrast to R, which denotes radius in cylindrical coordinates (R, ϕ, z).

surface brightness 25 magnitudes per square arcsec). To apply this model to the Galaxy, we take Θ_c equal to the local circular speed Θ_o and $R_{25} = 11.5$ kpc (de Vaucouleurs & Pence 1978), so that $r_{max} = 35$ kpc. Thus the minimal halo model suggests

$$M_G = 3.9 \times 10^{11} \left(\frac{\Theta_o}{220 \text{ km s}^{-1}} \right)^2 \left(\frac{r_{max}}{35 \text{ kpc}} \right) M_\odot. \quad 11.$$

Since the edge of the mass distribution and the edge of the H I distribution are not necessarily related, the minimal halo model is artificial. However, damped Lyman-α absorption systems in the spectra of high-redshift QSOs appear to arise from protogalactic disks whose radii are several times larger than the radii of optically visible Galactic disks (e.g. Turnshek et al 1989), and a galaxy resembling the minimal halo model might arise if low-mass stars were preferentially formed in the outer parts of these protogalactic disks.

3.3 *The Spherical Infall Model*

This model is motivated by a simple theoretical picture of galaxy formation. We assume that the Universe is filled with collisionless, cold, dark matter (i.e. matter with negligible cross-section, velocity dispersion, and luminosity) at the critical density given by

$$\rho_c(t) = (6\pi G t^2)^{-1}, \quad 12.$$

and that galaxies grow by the gravitational instability of a spectrum of initial density fluctuations. As a simple example of instability, we imagine that at time t_i an isolated seed mass M_0 is introduced into a Universe that is in unperturbed, pressureless Hubble flow. Because the density is critical, every mass element in the Universe is bound to the seed mass; the Hubble expansion of each element is gradually slowed and stopped (at the turnaround time). The mass element then falls back towards the seed to join its predecessors in a bound, growing, spherical structure that surrounds the seed. At any time $t \gg t_i$, the material that is just turning around is at the turnaround radius:

$$r_*(t) = \left(\frac{9GM_0}{2} \right)^{1/3} \left(\frac{4}{3\pi} \right)^{8/9} t_i^{-2/9} t^{8/9}. \quad 13.$$

A great simplification is that at times $t \gg t_i$, the structure around the seed mass grows self-similarly (Gunn 1977, Fillmore & Goldreich 1984, Bertschinger 1985). For example, the mass within a sphere of radius r surrounding the seed is

$$M(r,t) = \tfrac{4}{3}\pi\rho_c(t) r_*(t)^3 \mathcal{M}[r/r_*(t)], \qquad 14.$$

where $\mathcal{M}(x)$ is tabulated by Bertschinger (1985) and rises from 0 at $x = 0$ to $9\pi^2/16 = 5.55$ at $x = 1$ (turnaround). For $x \ll 1$, $\mathcal{M}(x) \simeq 11.2x^{3/4}$, so that for $r \ll r_*$,

$$M(r,t) = 11.2 \cdot \frac{2r_*^{9/4}}{9Gt^2} r^{3/4}$$

$$= 1.39 \frac{M_0^{3/4}}{G^{1/4} t_i^{1/2}} r^{3/4}. \qquad 15.$$

The second of Equations 15 shows that for $r \ll r_*(t)$ the mass distribution is time-independent, $M(r,t) \equiv M(r)$. Furthermore, the results can also be expressed in terms of the circular speed $\Theta_o = (GM(R_o)/R_o)^{1/2}$ at a given radius $R_o \ll r_*$:

$$M(r) = \frac{\Theta_o^2 R_o}{G} \left(\frac{r}{R_o}\right)^{3/4}, \quad r \ll r_*,$$

$$r_*(t) = 0.667 R_o^{1/9} (\Theta_o t)^{8/9},$$

$$M_0 = 0.648 \frac{\Theta_o^{8/3} R_o^{1/3} t_i^{2/3}}{G}. \qquad 16.$$

The circular speed well inside the turnaround radius is simply

$$\Theta(R) = \Theta_o (R_o/R)^{1/8}, \qquad 17.$$

which deviates from a flat rotation curve by less than 10% over a factor of two in radius. Thus the spherical infall model is consistent with observations that show the Galactic rotation curve to be nearly flat.

In this model, the total mass of the Galaxy is poorly defined; a natural but still arbitrary definition is the mass inside the turnaround radius,

$$M_* \equiv M[r_*(t), t] = 0.366 \frac{\Theta_o^{8/3} R_o^{1/3} t^{2/3}}{G} \qquad 18.$$

There are reasons for caution in applying this simple model to the Galaxy. First, the outer parts of the Galaxy are likely to be triaxial rather than spherical (see Section 2.4). Second, the approximation of spherical collapse around an isolated seed ignores the influence of our neighbor galaxy M31. Finally, the mass distribution in the inner regions may be distorted by the gravitational influence of the collisional baryonic component that sinks to the center of the collisionless structure as the baryons cool (Barnes 1987).

If, despite these warnings, we apply Equations 16 and 18 to the Galaxy, taking R_o and Θ_o to be the solar radius and local circular speed, we find

$$r_* = 807\,\mathrm{kpc}\left(\frac{t}{10^{10}\,\mathrm{yr}}\right)^{8/9}\left(\frac{R_o}{8.5\,\mathrm{kpc}}\right)^{1/9}\left(\frac{\Theta_o}{220\,\mathrm{km\,s^{-1}}}\right)^{8/9} \quad \text{and}$$

$$M_* = 1.44\times 10^{12} M_\odot\left(\frac{t}{10^{10}\,\mathrm{yr}}\right)^{2/3}\left(\frac{R_o}{8.5\,\mathrm{kpc}}\right)^{1/3}\left(\frac{\Theta_o}{220\,\mathrm{km\,s^{-1}}}\right)^{8/3}. \qquad 19.$$

The estimates of r_* and M_* should not be taken too seriously: The distance to M31 is only 725 kpc, thus the spherical approximation fails well before the turnaround radius. Nevertheless, the spherical infall model offers a plausible analytic model of the mass distribution in the outer Galaxy for $r \ll r_*$.

4. MASS ESTIMATES FROM STARS AND CLUSTERS

4.1 *Escape Speed*

If we approximate the Galaxy as an isolated stationary mass distribution and assume that all stars near the Sun are bound to the Galaxy, then the highest stellar velocity observed in the solar neighborhood must be less than the local escape speed $v_e \equiv [-2\Phi(R_o)]^{1/2}$, where Φ is the potential.

Several issues must be addressed in using this method:

1. Limited sample size. The phase-space density of stars near the escape speed is low; thus even in a large sample the largest observed velocity underestimates the escape speed (sample size bias).
2. Velocity errors. Although stellar radial velocities are now quite accurate, the proper motions and distances needed to determine the tangential velocity can have substantial errors. These errors lead to an overestimate of the escape speed (velocity error bias). If the actual escape speed is v_e and the typical velocity error is $\pm\Delta v$, the estimated escape speed based on the highest velocity star will be roughly $v_e + \Delta v$. This bias is illustrated by Cudworth's (1990) remeasurement of the proper motions of the highest velocity stars in the Carney et al (1988) sample, which lowered eight of the ten velocities.
3. Local Group interlopers. The sample may be contaminated by unbound stars from elsewhere in the Local Group (Dawson & de Robertis 1988). However, a spatially uniform population of the required density would be inconsistent with local star counts (Alexander 1982, Leonard & Tremaine 1990) and hence is probably not present.
4. Escaping stars. Stars can be accelerated to escape speed by a variety of

Table 1 Estimates of the local escape speed

Paper	Data base	Assumed Θ_o (km s^{-1})	v_e (km s^{-1})
Oort (1928)	Oort (1926)	–	Θ_o+63
Isobe (1974)	Eggen (1964)	272	377
Caldwell & Ostriker (1981)	Eggen (1964)	225	640 ± 100
Alexander (1982)	Eggen (1964) + Carney (1979)	220	>400
Sandage & Fouts (1987)	own compilation	220	>450
Carney et al (1988)	own compilation	220	>500
Cudworth (1990)	Carney et al (1988) +own proper motions	220	>475
Leonard & Tremaine (1990)	Carney et al (1988)	220	450–650

processes, both well-understood [e.g. encounters between field stars and hard binaries in globular clusters (Leonard & Duncan 1990)] and speculative [e.g. binary encounters deep in the potential well of a massive black hole at the Galactic center (Hills 1988)]. However, in order to have even one such star within the typical survey radius of 200 pc, roughly 10^8 such stars must have been ejected over the lifetime of the Galaxy. Such an ejection rate would be difficult to sustain: For example, it far exceeds the total stellar mass in all globular clusters or the upper limit to the mass of any black hole in the Galactic center.

Oort (1928) pointed out that no known stars with well-determined velocities relative to the Galactic center exceeded Θ_o+63 km s^{-1}. He suggested that this limit might be the local escape speed. Schmidt's (1965) mass model had a much larger difference of $v_e-\Theta_o=130$ km s^{-1} ($\Theta_o=250$ km s^{-1}, $v_e=380$ km s^{-1}), implying that few or no visible stars were close to the escape energy. More recent proper motion and radial velocity surveys have discovered stars with higher velocities and hence yield larger estimates of the local escape speed (Table 1).

By using a power-law fit to extrapolate the cumulative distribution function of stellar velocities, Caldwell & Ostriker (1981) were the first to correct for sample size bias. Unfortunately, their extrapolation procedure is physically unrealistic.[5] They did not account for velocity error bias. Most subsequent authors account for sample size bias by simply quoting

[5] The use of a power law distribution is inappropriate because the density of stars should approach zero as $v \to v_e$; also, they identify v_e as the speed at which the cumulative distribution function is unity, leading to an escape speed that depends on sample size.

their result as a lower limit to the escape speed, and account for velocity error bias by arbitrarily eliminating the two or three highest-velocity stars from their sample. A conservative approach to velocity error bias is to discard the proper motion data and use only radial velocities; in this case the highest known velocity is 430 km s^{-1} for the star G166-37.

Leonard & Tremaine (1990) attempted to treat the sample size and velocity error biases consistently. They assume that the tangential velocity errors are Gaussian and that the velocity distribution near escape speed is of the form $n(v)dv \propto v^2(v_e - v)^k dv$, with exponent k in the range 0 to 2. They find that estimates of the escape speed are strongly correlated with the assumed exponent k and with the assumed velocity errors. Estimates from radial velocities alone are as accurate as estimates that use proper motions as well, and lead to

$$450\,\mathrm{km\,s^{-1}} < v_e < 650\,\mathrm{km\,s^{-1}}, \qquad 20.$$

with a 90% confidence interval.

In the WYSIWYG model, most of the mass is interior to the Sun so that $\Phi(r) \simeq -GM/r$ for $r \gtrsim R_o$. Thus the local escape speed is

$$v_e \simeq \sqrt{2}\Theta_o, \qquad 21.$$

which equals 311 km s^{-1} for a local circular speed $\Theta_o = 220$ km s^{-1} and is inconsistent with the data.

The escape speed in the minimal halo model (Equation 10) is

$$v_e = \Theta_o\{2[\ln(r_{max}/R_o) + 1]\}^{1/2}, \qquad 22.$$

which equals 484 km s^{-1} for $\Theta_o = 220\,\mathrm{km\,s^{-1}}$, $R_o = 8.5$ kpc, and $r_{max} = 35$ kpc, near the lower end of the allowable range (Equation 20).

The escape speed in the spherical infall model can be computed using $d\Phi/dr = -GM(r)/r^2$ and Equation 16.[6] We find

$$v_e = \sqrt{8}\Theta_o, \qquad 23.$$

which equals 622 km s^{-1} if $\Theta_o = 220$ km s^{-1}, near the upper end of the allowable range (Equation 20).

4.2 *Globular Clusters*

Shapley (1918) recognized that the overall shape and orientation of the Galaxy is outlined by the distribution of globular clusters on the sky. It is natural to hope that the overall mass distribution is also reflected in the kinematics of the globular cluster system. Over 150 clusters are known

[6] The calculation is approximate because Equation 16 for $M(r)$ is only valid for $r \ll r_*$, but should be fairly accurate since most of the contribution to $\Phi(R_o)$ comes from small radii.

(see Webbink 1985 for a compilation), and radial velocities have been measured for over 75% of these (e.g. Hesser et al 1986). The present sample of clusters is thus nearly complete and substantial improvements in the data are unlikely in the near future.[7]

Many authors have analyzed the kinematics and spatial structure of the Galactic globular cluster system, including Kurth (1950), von Hoerner (1955), Kinman (1959), Arp (1965), Woltjer (1975), Harris (1976), Hartwick & Sargent (1978), Clube & Watson (1979), Frenk & White (1980, 1982), Lynden-Bell & Frenk (1981), and Thomas (1989).

There are two natural approaches to analyzing the dynamics of a population of test particles such as globular clusters; local and global methods. We describe both for the case in which the Galactic potential Φ and the distribution of particles are spherically symmetric.

LOCAL METHOD The collisionless Boltzmann equation for a stationary spherical system reads (e.g. Binney & Tremaine 1987, Chapter 4):

$$\frac{d(\nu\overline{v_r^2})}{dr} + \frac{2\nu}{r}(\overline{v_r^2} - \overline{v_t^2}) = -\nu\frac{d\Phi}{dr}, \qquad 24.$$

where $\nu(r)$ is the number density of test particles at radius r, $\overline{v_r^2}(r)$ is the mean square radial velocity, and $v_t^2(r)$ is the mean square velocity in any direction perpendicular to the radius vector (the system is assumed to be spherically symmetric in all its properties so that v_t^2 is independent of the chosen perpendicular direction). The shape of the velocity dispersion tensor is specified by the anisotropy parameter

$$\beta(r) \equiv 1 - \overline{v_t^2}/\overline{v_r^2}; \qquad 25.$$

$\beta = 1$ for radial orbits, and $\beta = 0$ for isotropic orbits (i.e. orbits that combine to produce an isotropic velocity distribution). Numerical simulations of the formation of stellar systems through spherical collapse (see e.g. Aguilar & Merritt 1990) suggest that β rises from zero near the center to one in the outer parts.

The distribution of test particles in radius and velocity can be fit to simple fitting functions for $\nu(r)$, $v_r^2(r)$, and $\overline{v_t^2}(r)$. These functions can be substituted into Equation 24 to determine $d\Phi/dr$ and hence the mass distribution. Unfortunately, with less than 150 clusters it is difficult to determine more than one or two free parameters for each fitting function. For example, Frenk & White (1980) fit all three functions, ν, $\overline{v_r^2}$, and v_t^2 to power laws (two free parameters per function). Thomas (1989) used func-

[7] A few proper motions of nearby clusters have become available (Tucholke et al 1988).

tions with more free parameters, but the extra generality comes at the cost of strong correlations between the best-fit values of the parameters.

GLOBAL METHOD Here we assume that the cluster sample is complete—or at least that the incompleteness is not position-dependent—so that an average over observed clusters is equivalent to an average over orbital phase (both of which we denote with angle brackets $\langle\ \rangle$). Thus, for example, if the clusters orbit a point mass M, $\langle v^2 r^{1+p}\rangle\langle r^q\rangle^{-p/q}$ has dimensions of GM and can be used to estimate M. The virial theorem $\langle v^2\rangle\langle 1/r\rangle^{-1} = GM$ corresponds to $p = q = -1$; mass estimators based on $\langle v^2 r\rangle$ (Bahcall & Tremaine 1981, Lynden-Bell et al 1983, Heisler et al 1985) correspond to $p = 0$; and Kinman (1959) uses $p = -1$, $q = 1$. The estimated M depends on the assumed shape of the velocity dispersion tensor for all estimators except the virial theorem.

The method can also be applied to other potentials. For example, in the singular isothermal potential $\Phi(r) = \Theta_c^2 \ln r$ (which gives rise to a flat rotation curve with circular speed Θ_c), we have the simple result $\langle v^2\rangle = \Theta_c^2$ for any stationary spherical distribution of test particles. [Lynden-Bell & Frenk (1981) use this result to estimate Θ_o.] As in the case of the virial theorem for point masses, the result is independent of the shape of the velocity dispersion tensor.

Attempts to constrain the mass distribution from globular cluster kinematics are plagued by the unknown value of the anisotropy parameter β. The following argument shows that the anisotropy parameter can be determined in principle if accurate distances are available. The distances to the cluster and the Galactic center, together with the position of the cluster on the sky, can be used to derive the angle ϕ between the Sun and the Galactic center as seen from the cluster. Then (for example) if the clusters are on radial orbits, the line-of-sight velocity after subtracting the component resulting from the solar velocity should be maximized if $\phi = 0$ or π and zero if $\phi = \frac{1}{2}\pi$, while if the orbits are isotropic the rms line-of-sight velocity should be independent of ϕ. However, distance errors lead to errors in ϕ, especially for clusters near the Galactic center, and hence tend to isotropize the apparent velocity dispersion tensor. Thus, although the globular cluster dispersion tensor appears to be isotropic for $r \lesssim R_o$, the isotropy may result from large distance errors.[8]

The anisotropy is also difficult to determine for distant clusters: In this case the line-of-sight velocity has mainly a radial component (the angle ϕ is near zero), so there is no observational access to the tangential velocity.

[8] The distance errors can be estimated by requiring that no "finger of God" be pointing to us in the three-dimensional cluster distribution; in this way it can be shown that the rms fractional distance error exceeds 30% (Thomas 1989).

The observed line-of-sight dispersion is larger for $r > R_0$ than for $r < R_0$ but whether this reflects an increase in the overall dispersion ($\overline{v_r^2}$ and $\overline{v_t^2}$ both increasing, β roughly constant) or increasing anisotropy ($\overline{v_r^2}$ increasing, $\overline{v_t^2}$ decreasing, β approaching unity) is unknown.

In view of these problems, it is not surprising that globular clusters do not provide strong constraints on the mass distribution in the Galaxy. Thomas (1989) carried out successful fits to the cluster kinematics in which the ratio of the circular speed at $4.2R_0$ to the circular speed at R_0 varies from 1.2 to 0.9; for comparison, the WYSIWYG model predicts 0.48, the minimal halo model 1.0, and the spherical infall model 0.83. The limited data set probably leads to uncertainties of at least ± 0.1 in this ratio; thus the results are consistent with the minimal halo and spherical infall models, but inconsistent with the WYSIWYG model. Previously, Kinman (1959) tentatively concluded that the globular cluster kinematics were inconsistent with the WYSIWYG model. This result is perhaps the first dynamical evidence for substantial dark mass in our Galaxy.

4.3 *Kinematics of Distant Stars*

The Galaxy contains a spheroidal distribution of metal-weak stars whose density falls off roughly as $r^{-3.5}$ [see Freeman (1987) and Gilmore et al (1989) for reviews]. Surveys of the prominent members of this population (K giants, blue horizontal branch stars, and RR Lyrae variables) can probe the distribution of mass in the Galaxy out to several tens of kpc.

The line-of-sight velocity dispersion of the spheroid stars is roughly constant out to at least 25 kpc from the Sun (e.g. Ratnatunga & Freeman 1989). The measurements are consistent with a model in which the velocity dispersion tensor is independent of position, with principal axes along the axes of a cylindrical coordinate system, and dispersions equal to their values in the solar neighborhood: $(\overline{v_R^2}, \overline{v_\phi^2}, \overline{v_z^2}) = (140, 100, 76)$ km s^{-1} (Bahcall & Casertano 1986). Unfortunately these results are difficult to reconcile with simple dynamical models of a spherical stellar distribution; the basic problem is that the z-velocities are too low for the stars to rise far above the Galactic plane, leading to a flattened distribution (axis ratio ≈ 0.4) that contradicts the 0.6 axis ratio found from the star counts (Ratnatunga & Freeman 1985, 1989, White 1989). Possibly, the star counts sample larger radii than the velocity measurements, and the flattening of the spheroid decreases with distance (Freeman 1987); another possibility is that the local value of $\overline{v_z^2}$ is too low because of contamination by a metal-weak disk component (Arnold 1990, Morrison et al 1990, Sommer-Larsen & Zhen 1990).

But even if we can reconcile the star counts and the kinematics, the distant spheroid stars will probably not provide strong constraints on the

mass distribution. Just as in the case of the globular clusters, disentangling radial gradients in the overall dispersion from gradients in the anisotropy will be difficult. A more optimistic outlook is that an understanding of the orbital structure of the spheroid stars will provide clues to the formation of the Galaxy and thus will indirectly improve our understanding of its mass distribution.

5. MASS ESTIMATES FROM LOCAL GROUP GALAXIES

5.1 *Distant Satellites*

Many authors have used satellite galaxies to probe the mass distribution of the outer Galaxy (Hartwick & Sargent 1978, Lynden-Bell et al 1983, Peterson 1985, Olszewski et al 1986, Little & Tremaine 1987, Lynden-Bell 1988, Peterson & Latham 1989, Zaritsky et al 1989). Table 2 lists the known galaxies within 300 kpc—somewhat less than half the distance to M31. We have also listed the globular clusters at distances exceeding 50 kpc; these should have similar orbits and can be added to the sample to improve the statistics. Early attempts to investigate kinematics of satellite galaxies were plagued by errors in the velocity measurements, and the analysis continues to suffer from limited statistics (there are only 14 objects in Table 2). Another problem is that we cannot measure the anisotropy parameter β (Equation 25); since the objects are all much more distant than the Sun from the Galactic center, we have no access to the tangential velocity components.

Several indirect arguments suggest that most or all of the objects in Table 2 are bound to the Galaxy. (*a*) The objects are strongly concentrated around the Galaxy (9 are between 50 and 100 kpc but only 3 are between 100 and 200 kpc, a volume eight times larger), although this concentration may partly result from incompleteness. (*b*) Similar concentrations of small early-type galaxies are seen around other giant galaxies (Binggeli et al 1990). (*c*) One can most easily explain the spatial structure and kinematics of the Magellanic Stream (Section 5.2) by assuming that the Stream was torn off the Magellanic Clouds during their previous pericenter passage. (*d*) Dwarf spheroidal galaxies in Table 2 may be formed from dwarf spiral or irregular galaxies through ram-pressure stripping by the Galactic halo gas or star formation induced by tidal shocks [see Kormendy (1987) or Binggeli et al (1990) for discussions]; if this model is correct, the absence of young stars suggests that the dwarfs have been in the vicinity of the Galaxy for some time. (*e*) Many of the satellites appear to lie near one or two great circles in the sky (Kunkel & Demers 1976, Lynden-Bell 1976a, 1976b, 1982a); the reason for this is unknown, but the uniform distribution

Table 2 Satellite galaxies and globular clusters between 50 and 300 kpc[a]

Object	v_{los} (km s^{-1})	r (kpc)	μ	ν
LMC+SMC	61	51	0.46	0.12
Ursa Minor	−88	65	1.22	0.27
Draco	−95	75	1.65	0.32
Sculptor	74	79	1.05	0.20
Carina	14	93	0.044	0.0074
Fornax	−34	140	0.39	0.048
Leo II	16	220	0.14	0.012
Leo I	177	230	17.5	1.48
Pal 14	166	75	5.02	0.98
Eridanus	−138	85	3.93	0.70
Pal 3	−59	95	0.80	0.13
NGC 2419	−26	98	0.16	0.026
Pal 4	54	108	0.77	0.11
AM-1	−42	117	0.50	0.070

[a] Line-of-sight velocity v_{los} and distance r are Galactocentric, computed assuming $\Theta_o = 220$ km s^{-1} and $R_o = 8.5$ kpc. Published velocity errors are always $\lesssim 15$ km s^{-1} and are $\lesssim 5$ km s^{-1} for most objects. The quantities $\mu = (v_{los}/\Theta_o)^2(r/R_o)$, $\nu = (v_{los}/\Theta_o)^2(r/R_o)^{1/4}$. Listed are galaxies and then globular clusters, each in order of increasing distance. Data from compilation by Zaritsky et al (1989).

of the satellites in azimuth suggests that their orbits have phase mixed over several periods.

For each object in Table 2 we have tabulated the dimensionless quantity $\mu \equiv (v_{los}/\Theta_o)^2(r/R_o)$. If the objects are bound, and the potential is that of a point mass ($\Phi = -GM_G/r$) at $r \gtrsim 50$ kpc, we must have $\mu < 2GM_G/(\Theta_o^2 R_o)$. The WYSIWYG model of the Galaxy (Equation 7) thus requires $\mu < 2f$, where f is close to unity, which is violated by Eridanus ($\mu = 3.9$), Pal 14 ($\mu = 5.0$), and Leo I ($\mu = 17.5$); thus the WYSIWYG model cannot be reconciled with the dynamics of the satellite galaxies.

The minimal halo model (Equation 10) with $r_{max} \lesssim 50$ kpc requires $\mu < 2r_{max}/R_o$, where we have taken the parameter Θ_c to be equal to the local circular speed Θ_o. For our standard value $r_{max} = 35$ kpc, this implies $\mu < 8.2$, a constraint that is violated only by Leo I. Thus, if Leo I is bound—and its distance and velocity are correct—the minimal halo model is ruled out, although a model with a somewhat more extended halo ($r_{max} \gtrsim 75$ kpc) would still be consistent with the data.

Once we assume a value for the anisotropy parameter, the data in Table 2 can be used to estimate the total mass. The sample (Table 2) is too small to estimate the run of number density or dispersion with radius, so we must use global methods (cf Section 4.2). Initially we assume a point-mass potential, in which case the simplest global estimators are based on $\langle \mu \rangle$, which equals $\frac{1}{2}GM_G/(\Theta_o^2 R_o)$ for radial orbits and $\frac{1}{4}GM_G/(\Theta_o^2 R_o)$ for isotropic orbits (Lynden-Bell et al 1983); with this estimator, the data in Table 2 yield $M_G = 4.6 \times 10^{11} M_\odot$ or $9.2 \times 10^{11} M_\odot$ for radial or isotropic orbits respectively. These results are strongly influenced by Leo I and would drop by a factor of 1.94 in its absence. A more elaborate approach, which also yields the statistical uncertainty in the mass estimate, is to use Bayes' theorem along with an assumed a priori distribution of M_G to determine the probability distribution of M_G given the observed μs (Little & Tremaine 1987). For isotropic orbits, this method yields a median estimate $M_G = 12.5 \times 10^{11} M_\odot$ with 90% confidence that M_G lies in the interval $[9.3\text{–}20.9] \times 10^{11} M_\odot$ (Zaritsky et al 1989). In this case, exclusion of Leo I reduces the median mass estimate by almost a factor of three.

The strong influence of Leo I leads to the suspicion that a point-mass potential does not provide an adequate description of the dynamics. For example, we have stated that adding Leo I increases $\langle \mu \rangle$ by a factor 1.94. The probability that this large an increase would occur from a single object in a sample of 14 can be estimated from the probability distribution of μ (Little & Tremaine 1987); this probability is only 0.005 for isotropic orbits and 0.0004 for radial orbits. Of course, posterior probability estimates of this kind are often misleading, but the possibility that Leo I is bound and the velocity and distance estimates are correct strongly hints that the kinematics of the Galaxy's satellites are inconsistent with any model whose mass is concentrated within about 50 kpc.

The spherical infall model implies that the satellites are on radial orbits and that for $r \ll r_*$ the mass distribution has the form $M(r) = (\Theta_o^2 R_o^{1/4}/G) r^{3/4}$ (Equation 16). These predictions should be treated cautiously for several reasons: (*a*) the distant satellites are probably disturbed by M31; (*b*) the inner satellites probably have substantial tangential velocity components that were excited by gravitational torques during the expansion and early collapse of the Galaxy; (*c*) tidal forces from the

Galaxy may destroy satellites that fall too close to the center of the Galaxy. If we set these concerns aside, then we can predict the kinematics of the satellites; we find that the probability that $v \equiv (v_{los}/\Theta_o)^2(r/R_o)^{1/4}$ lies in the interval $[v, v+dv]$ is $p(v)dv$, where

$$p(v) = \frac{1}{35 \cdot 32 \cdot \pi} \frac{(8-v)^{7/2}}{v^{1/2}}. \qquad 26.$$

The values of v in Table 2 can be compared with Equation 26: The median of the predicted distribution (Equation 26) is 0.42 compared to 0.13 in the 14 observed values, while the predicted mean is $\langle v \rangle = \frac{4}{5}$ compared to the observed mean of 0.32. Another approach is to regard the normalizing factor $\Theta_o^2 R_o^{1/4}$ used in defining v as a free parameter estimated by fitting the observed and theoretical distributions of $v_{los}^2 r^{1/4}$; using procedures from Little & Tremaine (1987), we find that $\Theta_o^2 R_o^{1/4}$ should be smaller than our assumed value of $(220 \text{ km s}^{-1})^2(8.5 \text{ kpc})^{1/4}$ by a factor 0.41 (the 90% confidence interval is [0.14, 0.6]).

Evidently the observed vs are 2–3 times smaller than the spherical infall model would predict. The discrepancy is present in both the nearby ($r < 100$ kpc) and distant satellites. Peebles et al (1989) saw a similar discrepancy in a numerical investigation of the Local Group in which the Galaxy was formed by infall, so the discrepancy does not result from our analytic approximations.[9] One explanation might be that the dissipational collapse that produced the disk enhanced the density in the inner Galaxy and thereby increased Θ_o (e.g. Salucci & Frenk 1989); however, there is no evidence for such an enhancement in the rotation curve, the globular cluster kinematics, or the Magellanic Stream (see below). Another possibility is that the dispersion tensor of the satellites is isotropic. In this case Equation 26 is replaced by $p(v) \propto (8-v)^{23/2} v^{-1/2}$; the mean of this distribution is $\langle v \rangle = \frac{4}{13} = 0.31$, almost exactly the same as the observed value of 0.32. Of course, in this case the assumption of radial infall that we used to derive the mass distribution (Equation 16) is no longer correct, and a different model for galaxy formation is required. Moore & Frenk (1990) have located a binary system that resembles the Local Group in an N-body simulation of a universe containing cold dark matter. They find that the distribution of halo velocities is in good agreement with the

[9] In the Peebles et al simulation, the satellite orbits are assumed to sample the orbits of the particles that comprise the halo mass. In this case Equation 26 does not apply because it was derived by integrating over a finite population of objects in virial equilibrium; the appropriate alternative is to examine the distribution of v at a given radius, which is given by $p(v) = (4\pi)^{-1}(8/v-1)^{1/2}$. The mean $\langle v \rangle$ in this case is 2 rather than $\frac{4}{5}$, so the discrepancy is even worse.

distribution of velocities in Table 2. Their result suggests that the spherical infall model is oversimplified, and that more sophisticated models of the formation of the Galactic halo may correctly predict the kinematics of the Galaxy's satellites.

5.2 *The Magellanic Stream*

The Magellanic Stream is a trail of neutral hydrogen that stretches in a great circle across more than 100° of arc, starting from the Magellanic Clouds and running over the South Galactic Pole. It probably consists of debris torn off the Clouds by tidal forces. By fitting simulations of the tidal stripping process to the observations of the Stream, we can constrain the orbit of the Clouds and the mass distribution in the Galaxy. The radial velocity varies smoothly and nearly linearly as a function of distance from the Clouds, reaching the remarkably high value of -200 km s^{-1} (Galactocentric frame) at the tip of the Stream farthest from the Clouds. Although the distance to the Stream is unknown, it must be large compared to R_0, otherwise the great circle shape would be spoiled by parallax resulting from the Sun's offset from the Galactic center.

The following arguments preview some of the conclusions from simulations of the formation and evolution of the Stream. Since the potential well of the Clouds is shallow compared to that of the Galaxy, the orbits of elements of the Stream should be similar to the orbits of the Clouds. The Stream velocity of up to 200 km s^{-1} is much larger than the radial velocity of the center of mass of the Clouds (61 km s^{-1} from Table 2). Thus if the orbits are similar, the Clouds must be near pericenter or apocenter and their orbit around the Galaxy must be quite eccentric. If the pericenter was much closer than the present distance of the Clouds (50 kpc), the two Clouds would probably not have survived as a bound unit. Thus the Clouds must now be near pericenter rather than apocenter. The Stream cannot be torn off at the present pericenter passage because it would not have enough time to spread out over 100°, so its material must have been removed at the previous passage some 2 Gyr ago. The maximum radial velocity in any bound Kepler orbit with pericenter q is $(\frac{1}{2}GM/q)^{1/2}$. For $q = 50$ kpc, the 200 km s^{-1} infall at the tip implies $M > 9 \times 10^{11} M_\odot$, which is already large enough to rule out the WYSIWYG or minimal halo models.

Numerical simulations (Murai & Fujimoto 1980, Lin & Lynden-Bell 1982) confirm all of these conclusions. Both sets of authors modeled the Galaxy by a mass distribution yielding a flat rotation curve similar to Equation 10 for the minimal halo model except that the outer radius r_{max} was much larger. The circular speeds required to fit the Stream kinematics were 250 km s^{-1} (Murai & Fujimoto 1980) or 244 ± 12 km s^{-1} (Lin &

Lynden-Bell 1982), both roughly consistent with the local circular speed $\Theta_o = 220$ km s^{-1}. The numerical experiments indicate that an extended halo out to at least $r_{max} = 70$ kpc is needed to fit the Stream kinematics; point-mass models do not yield acceptable fits. Although none of the simulations used the potential for the spherical infall model, its similarity to the successful models (circular speed $\propto r^{-1/8}$ compared to circular speed = constant) suggests that the spherical infall model will produce much better fits than either the WYSIWYG or minimal halo model with $r_{max} \lesssim 50$ kpc, both of which have point-mass potentials at the distance of the Stream.

All of these analyses assume that gravity is the only force acting on the Stream. The steep H I gradients at the leading edges of the Magellanic Clouds may be due to ram pressure from Galactic halo gas, which may also exert drag on the Stream; however, it is unlikely that any drag force is strong enough to affect the Stream except over many orbital periods.

A curious feature of the Stream is that its maximum velocity of 200 km s^{-1} is not only much larger than the radial velocity of the Clouds, but also much larger than the radial velocity of any satellite within 200 kpc. (The rms radial velocity of the 12 objects in Table 2 within 200 kpc is only 83 km s^{-1}.) Thus, if the orbit of the Clouds is similar to that of the Stream, it must be very different from the orbits of the other satellites. A possible explanation is given by Raychaudhury & Lynden-Bell (1989), who argue that M31 exerted a substantial torque on the Clouds and Stream early in their orbital history.

Measurement of the proper motion of the Magellanic Clouds would provide an extra constraint on their orbit that could greatly improve our confidence in using the Stream to constrain the mass distribution of the Galaxy.

5.3 *The Dynamics of the Local Group*

The Local Group and other groups of galaxies probably arose through the gravitational instability of small perturbations in the early Universe. By relating the present structure and kinematics of the Local Group to plausible models of the initial perturbations, we can constrain the distribution of mass within it.

The Kahn-Woltjer (1959) model (see also Peebles 1971, Gunn 1975, Lynden-Bell 1982b, and Einasto & Lynden-Bell 1982) approximates the Local Group as an isolated system of two point masses (the Galaxy and M31) with zero angular momentum. The Hubble expansion of the two masses was slowed and stopped by their mutual attraction, and the masses are now falling towards each other. Fitting the observed Galactocentric distance ($d = 725$ kpc) and radial velocity ($v = -123$ km s^{-1} for $\Theta_o = 220$

km s^{-1}) of M31 yields a single constraint relating the sum of the masses M_{LG} (i.e. the total mass of the Local Group) and the age of the Universe t_0. The constraint can be written in terms of the dimensionless parameters

$$\alpha \equiv \frac{vt_0}{d}, \quad \beta \equiv \frac{GM_{LG}t_0^2}{d^3}, \tag{27.}$$

in the parametric form

$$\alpha = \frac{\sin\eta(\eta - \sin\eta)}{(1-\cos\eta)^2}, \quad \beta = \frac{(\eta - \sin\eta)^2}{(1-\cos\eta)^3}, \tag{28.}$$

where η is the eccentric anomaly of the orbit. For t_0 in the range 10 to 20 Gyr, we find M_{LG} in the range $5.64 \times 10^{12} M_\odot$ to $3.33 \times 10^{12} M_\odot$.

These values for the Local Group mass are inconsistent with the WYSIWYG model (by a factor of at least 10) or the minimal halo model (by a factor of at least 4) if we assume that (*a*) the masses of M31 and the Galaxy are similar, and (*b*) most of the mass in the Local Group, like most of the luminosity, is concentrated in these two galaxies.

The Kahn-Woltjer model has shortcomings. It is unlikely that the two galaxies existed soon after the Big Bang as isolated objects with their present masses. A more plausible approach, which is a generalization of the spherical infall model, is to assume that the initial mass distribution consists of two seed masses that grow at the rate $M \propto t^{2/3}$ expected for an isolated mass concentration in a critical universe (we call this the two-seed infall model). In linear perturbation theory, the divergence of the velocity field around each mass is zero, so the density surrounding each mass remains uniform. If for simplicity we assume that the two seeds that will grow into the Galaxy and M31 are equal, and that the Local Group mass M_{LG} is the sum of the present masses of the two seeds, then we can show (Peebles et al 1989) that the parameters α and β are given by

$$\alpha = \frac{2}{3} + \frac{\tau}{y}\frac{dy}{d\tau}, \quad \beta = \frac{\tau^{2/3}}{y^3}, \tag{29.}$$

where $y(\tau)$ is the solution of the differential equation

$$\frac{d}{d\tau}\tau^{4/3}\frac{dy}{d\tau} = -\frac{1}{y^2}, \tag{30.}$$

subject to the boundary conditions $y(\tau \to 0) = 1$ and $(dy/d\tau)(\tau \to 0) = 0$. For t_0 between 10 and 20 Gyr, the resulting value of M_{LG} is between $6.02 \times 10^{12} M_\odot$ and $3.61 \times 10^{12} M_\odot$, less than 10% higher than the values given by the Kahn-Woltjer model (Equation 28). The estimates are similar

because most of the peculiar velocity develops recently, after the galaxies have grown to nearly their present masses.

In the two-seed infall model, the collapse that forms the Galaxy is closely related to the collapse of the Local Group, and hence observations of the Local Group can be used to predict the parameters of the inner parts of the Galaxy, which ought to be adequately described by the spherical infall model of Section 3.3. Thus we identify $\frac{1}{2}M_{\rm LG}$ with $\frac{3}{5}M_0(t_0/t_i)^{2/3}$, where M_0 is the seed mass for the Galaxy at initial time t_i. The factor $\frac{3}{5}$ arises because only this fraction of the initial perturbation is in the growing mode if the initial Hubble flow around the seed mass is unperturbed. Then using the third of Equations 16, we obtain

$$\Theta_0 = 145\,{\rm km\,s^{-1}}\left(\frac{M_{\rm LG}}{10^{12}M_\odot}\right)^{3/8}\left(\frac{10^{10}\,{\rm yr}}{t_0}\right)^{1/4}\left(\frac{8.5\,{\rm kpc}}{R_0}\right)^{1/8}. \qquad 31.$$

Using values of $M_{\rm LG}$ and t_0 from above, we find that Θ_0 lies between 283 km s^{-1} and 197 km s^{-1}, which nicely brackets the observed value of about 220 km s^{-1}.

This approximate analytic comparison can be checked by numerical simulations. Peebles et al (1989) have numerically followed the growth of two seed masses embedded in a cold critical universe until the parameter α equals the observed value for the Galaxy and M31. They find that $\Theta_0 = 259$ km s^{-1} ($t_0 = 7.8$ Gyr) or 191 km s^{-1} ($t_0 = 13.8$ Gyr), within 30% of the analytic estimates, which again brackets the observed value.

In the two-seed infall model, the mass of the Galaxy cannot be cleanly separated from the mass of M31: The turnaround surface, where the radial velocity relative to the center of symmetry of the Local Group is zero, encloses both galaxies. Peebles et al show that the total mass inside the turnaround surface is $4.9 \times 10^{12}M_\odot$ for $t_0 = 7.8$ Gyr and $3.5 \times 10^{12}M_\odot$ for $t_0 = 13.8$ Gyr.

These analyses assume that there are no external torques on the Local Group from other mass concentrations. Raychaudhury & Lynden-Bell (1989) have analyzed the time dependence of the external torques using the observed distribution of galaxies within 12 Mpc ($H = 55$ km s^{-1} Mpc^{-1}) and the plausible assumptions that (*a*) the mass-to-light ratios of other galaxies are the same as that derived for the Local Group using the Kahn-Woltjer model; (*b*) the universe is critical, so the scale factor $a(t) \propto t^{2/3}$; and (*c*) masses of galaxies grow as $t^{2/3}$ (as we have assumed already in the two-seed infall model). They find that the direction of M31 has swung through 19° since the Big Bang; the tidally induced angular momentum of the Local Group far exceeds the spin angular momenta of the visible disks of the Galaxy and M31; and the masses derived from the Kahn-Woltjer argument are not substantially affected.

A challenging test of these models is whether they can predict the velocities of the dwarf galaxies in the outer parts of the Group. Peebles et al show that the two-seed infall model predicts the velocities of most of these galaxies with adequate accuracy (error $\lesssim 50$ km s^{-1}), but only if the Universe is younger ($t_0 = 7.8$ Gyr) than current ages from stellar evolution. In addition, the model predicts that NGC 6822 is approaching the Galaxy at 87 km s^{-1}, while in fact it is receding at 44 km s^{-1}. Mishra (1985) has also carried out a detailed analysis of the orbits of small galaxies in the Local Group using the Kahn-Woltjer model. Mishra does find orbits for NGC 6822 that fit the observations, but only if it passes within 30 kpc of the Galaxy, in which case his approximation that the Galaxy is a point mass is suspect.

A very promising approach to the study of the Local Group is through cosmological N-body simulations, by isolating and analyzing groups in the simulations that resemble the Local Group. Moore & Frenk (1990) and Kroeker & Carlberg (1990) have found analogs to the Local Group in simulations of cold dark matter universes. Both groups find that the Kahn-Woltjer estimate of the group mass is lower than the "actual" mass (defined as the sum of the masses in two spheres around each galaxy that extend to the center of mass) by about a factor of two.

6. SUMMARY

Several dynamical tests establish that most of the mass in our Galaxy and other disk galaxies lies outside the distribution of visible stars, in a so-far invisible halo component. However, the shape and extent of the halo remain uncertain. A conservative model is the minimal halo (Section 3.2), in which the halo extends to $r_{\max} \approx 35$ kpc and the total mass is $M_G \approx 4 \times 10^{11} M_\odot$. This minimal Galaxy is consistent with measurements of the rotation curve, the local escape speed, the kinematics of the globular cluster system, and the kinematics of most satellite galaxies. However, the model cannot explain the observed radial velocity of Leo I, or the dynamics of the Magellanic Stream or Local Group. Advocates of a minimal Galaxy can argue that Leo I is not bound, that the Magellanic Stream may be affected by nongravitational forces, and that most of the Local Group mass may be attached to M31 rather than the Galaxy.

Galaxy formation through gravitational instability of cold collisionless dark matter naturally produces extended dark halos. A simple example is spherical infall of cold matter onto a central seed mass (Section 3.3). The spherical infall model, generalized to infall onto two seed masses when one treats the dynamics of the Local Group, is consistent with all the observations, with one possible exception. The observed velocities of sat-

ellite galaxies appear to be too low by a factor of about 1.6, if, as the model predicts, the satellites are on near-radial orbits. The observations are probably consistent with more general infall models in which external torques are strong enough to isotropize the velocity distribution of the satellites.

In the infall model the total mass of the Galaxy is ill-defined. The total mass of the Local Group inside the turnaround surface is in the range (3–6) $\times 10^{12} M_{\odot}$.

A model based on radial infall onto a seed mass is appropriate if galaxies form by accretion of cold matter onto seeds such as black holes or cosmic string loops. However, the model is less reliable if structure develops from cold matter subject to Gaussian density fluctuations, which generally produce pancakes or a clustering hierarchy. It is important to investigate whether numerical simulations of structure formation from cold matter and Gaussian fluctuations, or other cosmological scenarios, can produce models of the Galaxy that agree with the observed kinematics of the satellite galaxies, the Magellanic Stream, and the Local Group.

ACKNOWLEDGMENTS

We thank Ray Carlberg, Konrad Kuijken, George Lake, Blane Little, Paul Schechter, and Peter Thomas for discussions and advice during the preparation of this review. Financial support was provided by operating grants from NSERC.

Literature Cited

Aaronson, M., Blanco, V. M., Cook, K. H., Schechter, P. L. 1989. *Ap. J. Suppl.* 70: 637

Aaronson, M., Blanco, V. M., Cook, K. H., Olszewski, E. W., Schechter, P. L. 1990. *Ap. J. Suppl.* 73: 841

Aguilar, L. A., Merritt, D. 1990. *Ap. J.* 354: 33

Alexander, J. B. 1982. *MNRAS* 201: 579

Arnold, R. 1990. *MNRAS* 244: 465

Arp, H. C. 1965. In *Galactic Structure*, ed. A. Blaauw, M. Schmidt p. 401. Chicago: Univ. of Chicago Press. 606 pp.

Bahcall, J. N. 1986. *Annu. Rev. Astron. Astrophys.* 24: 577

Bahcall, J. N., Casertano, S. 1986. *Ap. J.* 308: 347

Bahcall, J. N., Schmidt, M., Soneira, R. M. 1983. *Ap. J.* 265: 730

Bahcall, J. N., Soneira, R. M. 1980. *Ap. J. Suppl.* 44: 73

Bahcall, J. N., Tremaine, S. 1981. *Ap. J.* 244: 805

Bardeen, J. M., Bond, J. R., Kaiser, N., Szalay, A. S. 1986. *Ap. J.* 304: 15

Barnes, J. E. 1987. In *Nearly Normal Galaxies*, ed. S. M. Faber, p. 154. New York: Springer. 464 pp.

Berendzen, R., Hart, R., Seeley, D. 1984. *Man Discovers the Galaxies.* New York: Columbia Univ. Press. 228 pp.

Bertschinger, E. 1985. *Ap. J. Suppl.* 58: 39

Binggeli, B., Tarenghi, M., Sandage, A. 1990. *Astron. Astrophys.* 228: 42

Binney, J. 1987. In *The Galaxy*, ed. G. Gilmore, R. Carswell, p. 399. Dordrecht: Reidel. 435 pp.

Binney, J., Tremaine, S. 1987. *Galactic Dynamics.* Princeton: Princeton Univ. Press. 719 pp.

Blitz, L. 1979. *Ap. J. Lett.* 231: L115

Blitz, L., Fich, M., Stark, A. A. 1980. In

Interstellar Molecules, IAU Symp. No. 87, ed. B. Andrew, p. 213. Dordrecht: Reidel. 704 pp.
Blitz, L., Fich, M., Stark, A. A. 1982. *Ap. J. Suppl.* 49: 183
Blitz, L., Spergel, D. N. 1991. *Ap. J.* 370: 205
Bucerius, H. 1934. *Astron. Nachr.* 259: 365
Burton, W. B. 1988. In *Galactic and Extragalactic Radio Astronomy*, ed. G. L. Verschuur, K. I. Kellerman, p. 295. New York: Springer. 2nd cd.
Burton, W. B., Gordon, M. A. 1978. *Astron. Astrophys.* 63: 7
Caldwell, J. A. R., Coulson, I. M. 1987. *Astron. J.* 93: 1090
Caldwell, J. A. R., Ostriker, J. P. 1981. *Ap. J.* 251: 61
Camm, G. L. 1938. *MNRAS* 99: 71
Carney, B. W. 1979. *Ap. J.* 233: 877
Carney, B. W., Latham, D. W., Laird, J. B. 1988. *Astron. J.* 96: 560
Casertano, S., van Albada, T. S. 1990. In *Baryonic Dark Matter*, ed. D. Lynden-Bell, G. Gilmore, p. 159. Dordrecht: Kluwer. 298 pp.
Chini, R., Wink, J. E. 1984. *Astron. Astrophys.* 139: L5
Clemens, D. P. 1985. *Ap. J.* 295: 422
Clube, S. V. M., Watson, F. G. 1979. *MNRAS* 187: 863
Cudworth, K. M. 1990. *Astron. J.* 99: 590
Dawson, P. C., de Robertis, M. M. 1988. In *The Mass of the Galaxy*, ed. M. Fich, p. 21. Toronto: Can. Inst. Theoret. Astrophys. 68 pp.
de Vaucouleurs, G., Pence, W. D. 1978. *Astron. J.* 83: 1163
Dubath, P., Mayor, M., Burki, G. 1988. *Astron. Astrophys.* 205: 77
Eggen, O. J. 1964. *R. Obs. Bull.* No. 84
Einasto, J., Lynden-Bell, D. 1982. *MNRAS* 199: 67
Fich, M., Blitz, L., Stark, A. A. 1989. *Ap. J.* 342: 272
Fich, M., Silkey, M. 1991. *Ap. J.* 366: 107
Fillmore, J. A., Goldreich, P. 1984. *Ap. J.* 281: 9
Freeman, K. C. 1987. *Annu. Rev. Astron. Astrophys.* 25: 603
Frenk, C. S., White, S. D. M. 1980. *MNRAS* 193: 295
Frenk, C. S., White, S. D. M. 1982. *MNRAS* 198: 173
Georgelin, Y. P., Georgelin, Y. M. 1970. *Astron. Astrophys.* 8: 117
Gilmore, G., King, I. R., van der Kruit, P. C. 1990. In *The Milky Way as a Galaxy*, Saas-Fee Advanced Course No. 19, ed. R. Buser, I. R. King. Mill Valley: Univ. Sci. Books
Gilmore, G., Wyse, R. F. G., Kuijken, K. 1989. *Annu. Rev. Astron. Astrophys.* 27: 555
Gunn, J. E. 1975. *Comments Astrophys. Space Phys.* 6: 7
Gunn, J. E. 1977. *Ap. J.* 218: 592
Gwinn, C. R., Moran, J. M., Reid, M. J., Schneps, M. H., Genzel, R., Downes, D. 1989. In *The Center of the Galaxy IAU Symp. No. 136*, ed. M. Morris, p. 47. Dordrecht: Kluwer. 661 pp.
Hanson, R. B. 1987. *Astron. J.* 94: 409
Hanson, R. B. 1988. In *Mapping the Sky IAU Symp. No. 133*, ed. S. Debarbat, J. A. Eddy, H. K. Eichhorn, A. P. Upgren, p. 275. Dordrecht: Kluwer. 512 pp.
Harris, W. E. 1976. *Astron. J.* 81: 1095
Hartwick, F. D. A., Sargent, W. L. W. 1978. *Ap. J.* 221: 512
Heisler, J., Tremaine, S., Bahcall, J. N. 1985. *Ap. J.* 298: 8
Hesser, J. E., Shawl, S: J., Meyer, J. E. 1986. *Publ. Astron. Soc. Pac.* 98: 403
Hills, J. G. 1988. *Nature* 331: 687
Hron, J. 1987. *Astron. Astrophys.* 176: 34
Hron, J. 1989. *Astron. Astrophys.* 222: 85
Innanen, K. A. 1973. *Astrophys. Space Sci.* 47: 299
Isobe, S. 1974. *Astron. Astrophys.* 36: 327
Jackson, P. D., FitzGerald, M. P., Moffat, A. F. J. 1979. In *The Large Scale Characteristics of the Galaxy, IAU Symp. No. 84*, cd. W. B. Burton, p. 221. Dordrecht: Reidel. 611 pp.
Kahn, F. D., Woltjer, L. 1959. *Ap. J.* 130: 705
Kapteyn, J. C. 1922. *Ap. J.* 55: 302
Kerr, F. J. 1962. *MNRAS* 123: 327
Kerr, F. J. 1964. In *The Galaxy and the Magellanic Clouds, IAU Symp. No. 20*, ed. F. J. Kerr, A. W. Rodgers, p. 81. Canberra: Austral. Acad. Sci. 393 pp.
Kerr, F. J., Lynden-Bell, D. 1986. *MNRAS* 221: 1023
Kinman, T. D. 1959. *MNRAS* 119: 559
Knapp, G. R. 1988. In *The Outer Galaxy*, ed. L. Blitz, F. J. Lockman, p. 3. New York: Springer. 291 pp.
Kormendy, J. 1987. In *Nearly Normal Galaxies*, ed. S. M. Faber, p. 163. New York: Springer. 464 pp.
Kroeker, T. L., Carlberg, R. G. 1990. Preprint
Kuijken, K. 1991. In *Warped Disks and Inclined Rings around Galaxies*, ed. F. Briggs, S. Casertano, P. Sackett. Cambridge: Cambridge Univ. Press. In press
Kunkel, W. E., Demers, S. 1976. *R. Greenwich Obs. Bull. No. 182*: 241
Kurth, R. 1950. *Z. Astrophys.* 28: 60
Kwee, K. K., Muller, C. A., Westerhout, G. 1954. *Bull. Astron. Inst. Neth.* 12: 211
Leonard, P. J. T., Duncan, M. J. 1990. *Astron. J.* 99: 608

Leonard, P. J. T., Tremaine, S. 1990. *Ap. J.* 353: 486
Lewis, J. R. 1990. *MNRAS* 244: 247
Lin, C. C., Mestel, L., Shu, F. H. 1965. *Ap. J.* 142: 1431
Lin, D. N. C., Lynden-Bell, D. 1982. *MNRAS* 198: 707
Lindblad, B. 1926. *Upsala Medd.* No. 3
Little, B., Tremaine, S. 1987. *Ap. J.* 320: 493
Lynden-Bell, D. 1976a. *MNRAS* 174: 695
Lynden-Bell, D. 1976b. *R. Greenwich Obs. Bull. No. 182*: 235
Lynden-Bell, D. 1982a. *Observatory* 102: 202
Lynden-Bell, D. 1982b. In *Astrophysical Cosmology*, ed. H. A. Brück, G. V. Coyne, M. S. Longair, p. 86. Vatican City: Pontifical Acad. Sci. 600 pp.
Lynden-Bell, D. 1988. In *The Outer Galaxy*, ed. L. Blitz, F. J. Lockman, p. 18. Berlin: Springer. 291 pp.
Lynden-Bell, D., Frenk, C. S. 1981. *Observatory* 101: 200
Lynden-Bell, D., Cannon, R. D., Godwin, P. J. 1983. *MNRAS* 204: 87
Mihalas, D., Binney, J. 1981. *Galactic Astronomy*. San Francisco: Freeman. 597 pp.
Mishra, R. 1985. *MNRAS* 212: 163
Moffat, A. F. J., FitzGerald, M. P., Jackson, P. D. 1979. *Astron. Astrophys. Suppl.* 38: 197
Moore, B., Frenk, C. 1990. In *Dynamics and Interactions of Galaxies*, ed. R. Wielen, p. 410. Berlin: Springer. 518 pp.
Morrison, H. L., Flynn, C., Freeman, K. C. 1990. *Astron. J.* 100: 1191
Murai, T., Fujimoto, M. 1980. *Publ. Astron. Soc. Jpn.* 32: 581
Olszewski, E. W., Peterson, R. C., Aaronson, M. 1986. *Ap. J. Lett.* 302: L45
Oort, J. H. 1926. *Publ. Kapteyn Astron. Lab.* No. 40
Oort, J. H. 1927. *Bull. Astron. Inst. Neth.* 3: 275
Oort, J. H. 1928. *Bull. Astron. Inst. Neth.* 4: 269
Paul, E. R. 1986. *J. Hist. Astron.* 17: 155
Pecker, J.-C., ed. 1964. *Trans. IAU*, 12B: 315
Peebles, P. J. E. 1971. *Physical Cosmology*. Princeton: Princeton Univ. Press. 282 pp.
Peebles, P. J. E. 1986. *Nature* 321: 27
Peebles, P. J. E., Melott, A. L., Holmes, M. R., Jiang, L. R. 1989. *Ap. J.* 345: 108
Perek, L. 1962. *Adv. Astron. Astrophys.* 1: 165
Peterson, R. C. 1985. *Ap. J.* 297: 309
Peterson, R. C., Latham, D. W. 1989. *Ap. J.* 336: 178
Petrovskaya, I. V., Teerikorpi, P. 1986. *Astron. Astrophys.* 163: 39
Plaskett, J. S., Pearce, J. A. 1936. *Publ. Dom. Astrophys. Obs.* 5: 241
Racine, R., Harris, W. E. 1989. *Astron. J.* 98: 1609
Ratnatunga, K. U., Freeman, K. C. 1985. *Ap. J.* 291: 260
Ratnatunga, K. U., Freeman, K. C. 1989. *Ap. J.* 339: 106
Raychaudhury, S., Lynden-Bell, D. 1989. *MNRAS* 240: 195
Reid, M. J. 1989. In *The Center of the Galaxy, IAU Symp. No. 136*, ed. M. Morris, p. 37. Dordrecht: Kluwer. 661 pp.
Reid, M. J., Moran, J. M., Gwinn, C. R. 1988a. In *The Impact of VLBI on Astrophysics and Astronomy, IAU Symp. No. 129*, ed. M. J. Reid, J. M. Moran, p. 169. Dordrecht: Kluwer. 599 pp.
Reid, M. J., Schneps, M. H., Moran, J. M., Gwinn, C. R., Genzel, R., et al. 1988b. *Ap. J.* 330: 809
Rohlfs, K., Chini, R., Wink, J. E., Böhme, R. 1986. *Astron. Astrophys.* 158: 181
Rohlfs, K., Kreitschmann, J. 1988. *Astron. Astrophys.* 201: 51
Salucci, P., Frenk, C. S. 1989. *MNRAS* 237: 247
Sandage, A. R., Fouts, G. 1987. *Astron. J.* 93: 74
Sanders, R. H. 1990. *Astron. Astrophys. Rev.* 2: 1
Schechter, P., Aaronson, M., Cook, K. H., Blanco, V. M. 1988. In *The Outer Galaxy*, ed. L. Blitz, F. J. Lockman, p. 31. New York: Springer. 291 pp.
Schmidt, M. 1965. In *Galactic Structure*, ed. A. Blaauw, M. Schmidt, p. 513. Chicago: Univ. of Chicago Press. 606 pp.
Schmidt, M. 1985. In *The Milky Way Galaxy, IAU Symp. No. 106*, ed. H. van Woerden, R. J. Allen, W. B. Burton, p. 75. Dordrecht: Reidel. 660 pp.
Schneider, S. E., Terzian, Y. 1983. *Ap. J. Lett.* 274: L61
Shane, W. W., Bieger-Smith, G. P. 1966. *Bull. Astron. Inst. Neth.* 18: 263
Shapley, H. 1918. *Ap. J.* 48: 154
Shuter, W. L. H. 1982. *MNRAS* 199: 109
Sinha, R. P. 1978. *Astron. Astrophys.* 69: 227
Sommer-Larsen, J., Zhen, C. 1990. *MNRAS* 242: 10
Stebbins, J., Whitford, A. E. 1936. *Ap. J.* 84: 132
Strömberg, G. 1918. *Ap. J.* 47: 7
Strömberg, G. 1925. *Ap. J.* 61: 363
Swings, J.-P., ed. 1985. *Trans. IAU* 19B: 254
Thomas, P. 1989. *MNRAS* 238: 1319
Trumpler, R. J. 1930. *Publ. Astron. Soc. Pac.* 42: 211
Tucholke, H.-J., Brosche, P., Geffert, M. 1988. In *Globular Cluster Systems in Galaxies, IAU Symp. No. 126*, ed. J. E. Grindlay, A. G. D. Philip, p. 525. Dordrecht: Kluwer. 751 pp.
Turnshek, D. A., Wolfe, A. M., Lanzetta, K.

M., Briggs, F. H., Cohen, R. D., et al. 1989. *Ap. J.* 344: 567
van den Bergh, S. 1988. *Comments Astrophys.* 12: 131
von Hoerner, S. 1955. *Z. Astrophys.* 35: 255
Webbink, R. F. 1985. In *Dynamics of Star Clusters, IAU Symp. No. 113*, ed. J. Goodman, P. Hut, p. 541. Dordrecht: Reidel
Welch, D. W. 1988. In *The Mass of the Galaxy*, ed. M. Fich, p. 29. Toronto: Can. Inst. Theoret. Astrophys. 68 pp.
White, S. D. M. 1989. *MNRAS* 237: 51
Wielen, R., ed. 1990. *Dynamics and Interactions of Galaxies.* Berlin: Springer. 518 pp.
Woltjer, L. 1975. *Astron. Astrophys.* 42: 109
Zaritsky, D., Olszewski, E. W., Schommer, R. A., Peterson, R. C., Aaronson, M. 1989. *Ap. J.* 345: 759